



## Design and synthesis of membrane fusion inhibitors against the feline immunodeficiency virus

Shinya Oishi<sup>a,\*</sup>, Yasuyo Koderia<sup>a</sup>, Hiroki Nishikawa<sup>a</sup>, Hirotaka Kamitani<sup>a</sup>, Tsuyoshi Watabe<sup>a</sup>, Hiroaki Ohno<sup>a</sup>, Tadafumi Tochikura<sup>a</sup>, Kazuki Shimane<sup>b</sup>, Eiichi Kodama<sup>b,†</sup>, Masao Matsuoka<sup>b</sup>, Fuminori Mizukoshi<sup>c</sup>, Hajime Tsujimoto<sup>c</sup>, Nobutaka Fujii<sup>a,\*</sup>

<sup>a</sup> Graduate School of Pharmaceutical Sciences, Kyoto University, Sakyo-ku, Kyoto 606-8501, Japan

<sup>b</sup> Laboratory of Virus Control, Institute for Virus Research, Kyoto University, Sakyo-ku, Kyoto 606-8507, Japan

<sup>c</sup> Department of Veterinary Internal Medicine, Graduate School of Agricultural and Life Sciences, The University of Tokyo, 1-1-1 Yayoi, Bunkyo-ku, Tokyo 113-8657, Japan

### ARTICLE INFO

#### Article history:

Received 24 April 2009

Revised 30 May 2009

Accepted 2 June 2009

Available online 6 June 2009

#### Keywords:

Feline immunodeficiency virus

Fusion inhibitor

$\alpha$ -Helix

Heptad repeat

### ABSTRACT

Feline immunodeficiency virus (FIV) is a pathogenic virus that causes an AIDS-like syndrome in the domestic cats. For viral entry and infection, fusion between the virus and the cell membrane is the critical process and this process is mediated by an envelope glycoprotein gp40. We have identified fusion inhibitory peptides from the heptad repeat-2 (HR2) of gp40. Remodeling of the original sequences using  $\alpha$ -helix-inducible motifs revealed the interactive residues of gp40. Comparative analysis of HR2 peptides derived from four FIV strains demonstrated that the interactive surface of the Shizuoka strain-derived HR2 peptides provides the highest affinity of all the FIV strains examined.

© 2009 Elsevier Ltd. All rights reserved.

### 1. Introduction

Feline immunodeficiency virus (FIV) causes immunodeficiency in domestic cats. The prevalence is very high in many countries.<sup>1</sup> FIV shares a homologous replication cycle and pathological processes with human immunodeficiency virus (HIV) in which a progressive and irreversible depletion of CD4<sup>+</sup> T cells leads to an AIDS-like syndrome. FIV is horizontally transmitted by the exposure to virus contained in blood or saliva from infected cats and it can be vertically transmitted from queens to kittens, sharing similar transmission routes with HIV. Consequently, FIV has been used as an animal model for the development of anti-HIV agents.<sup>2</sup>

The cell entry process of viruses including receptor binding and membrane fusion is mediated by the envelope glycoproteins.<sup>3</sup> In the initial stage for productive infection, the FIV surface (SU) glycoprotein attaches to both CD134 and CXCR4.<sup>4</sup> The primary receptor of FIV is CD134 expressed on activated CD4<sup>+</sup> T cells in contrast that the primate lentiviruses target CD4. The co-receptor CXCR4 is targeted both by FIV and HIV.<sup>5</sup> The inhibitors of this process such as specific CXCR4 antagonists effectively suppress viral

replication.<sup>5b,6</sup> Fusion between the host cellular and viral membranes occurs through the rearrangement of the transmembrane (TM) glycoprotein gp40.<sup>7</sup> Although the detailed mechanism of the fusion process of FIV remains unresolved, the conservation of the gp40 ectodomain among the lentiviruses supports the class I membrane fusion reaction. The folding of two heptad repeats in gp40 leads to the formation of a trimer of hairpins with a central  $\alpha$ -helical coiled-coil that promotes membrane fusion. As recently observed in the successful development of an HIV fusion inhibitor, enfuvirtide,<sup>8</sup> the fusion process is another promising target for anti-FIV agents.<sup>9</sup>

Recently, we have reported the identification of two potent HIV fusion inhibitors by the remodeling of HIV-1 gp41-derived peptides.<sup>10</sup> Both peptides were designed by the stabilization of bioactive  $\alpha$ -helical conformations of C34 **1** and enfuvirtide, which inhibit the refolding process to produce the fusogenic six-helix bundle structure. Incorporation of the characteristic X-EE-XX-KK repeats (X: the original residue; E: Glu; K: Lys) into the gp41 heptad repeat-2 (HR2) peptides stabilized the  $\alpha$ -helix structure by the formation of potential electrostatic interaction between Glu at the *i* position and Lys at the *i* + 4 position. Such peptide stabilization resulted in improved anti-HIV activity. In addition, this approach simultaneously distinguished the indispensable residues located at the interactive surface from the less essential solvent accessible residues. These residues can be substituted for improving the aqueous solubility of the peptides. We speculate that this design

\* Corresponding authors. Tel.: +81 75 753 4551; fax: +81 75 753 4570.

E-mail addresses: [soishi@pharm.kyoto-u.ac.jp](mailto:soishi@pharm.kyoto-u.ac.jp) (S. Oishi), [nfujii@pharm.kyoto-u.ac.jp](mailto:nfujii@pharm.kyoto-u.ac.jp) (N. Fujii).

<sup>†</sup> Present address: Division of Emerging Infectious Diseases, Tohoku University School of Medicine, 2-1 Seiryochō, Aoba-ku, Sendai 980-8575, Japan.

concept should be applicable to anti-FIV peptides. Since there have been no previous reports on the interactive mode of FIV gp40 during the fusion process, this approach could identify novel potent anti-FIV peptides and disclose the interacting interface for further optimization.

Herein, we present the design, synthesis and bioevaluation of FIV HR2-derived peptides with  $\alpha$ -helix inducible motifs. On the basis of the appropriate anti-FIV sequence identified, the congeneric HR2 peptides from four FIV strains belonging to two different subtypes were comparatively evaluated for inhibitory activity against the fusion process by using an ELISA.

## 2. Results and discussion

### 2.1. Peptide design and synthesis

Peptide design began with two putative coiled-coil-like regions of FIV envelope protein gp40 identified by the LearnCoil-VMF program.<sup>11</sup> Alignment with two heptad repeats of HIV-1 gp41 identified the corresponding heptad repeat-1 (HR1) and HR2 regions in FIV gp40 (Fig. 1a).<sup>11</sup> The predicted C-terminal sequence **3a** coincides with a previously reported effective inhibitor of FIV infection, T1577,<sup>9b</sup> and shares four amino acids with HR2 of HIV-1 gp41. The potential  $\alpha$ -helical wheel of **3a** is depicted in Figure 1b. On the basis of the crystal structure of HIV-1 gp41 and the alignment with the HIV-1 sequence, it is assumed that residues at the *a*, *d* and *e* positions of peptide **3a** are involved in the interaction with the central coiled-coil of the HR1 trimer to form the six-helix bundle. On the other hand, residues at *b*, *c*, *f* and *g* positions may facilitate the stabilization of the bioactive secondary structure rather than directly interact with HR1. We designed a modified peptide **4a**, in which Glu and Lys were arranged for *b/c* and *f/g* positions of **3a**, respectively, in order to stabilize the  $\alpha$ -helix structure through the formation of consecutive salt bridges. In addition, two analogues **5** and **6** with shifted interactive surfaces were designed, in

which *a/b/e* and *a/d/g* positions were expected to interact with HR1, respectively.

All peptides were prepared by a standard protocol for Fmoc-based solid-phase peptide synthesis. The peptide resins were manually constructed using *N,N*-diisopropylcarbodiimide (DIC) and *N*-hydroxybenzotriazole (HOBt) on NovaSyn TGR resin. The peptide N-terminus was acetylated. The peptides were obtained by the treatment with the deprotection cocktail [TFA/thioanisole/*m*-cresol/1,2-ethanedithiol/H<sub>2</sub>O (80:5:5:5:5)] followed by HPLC purification. The peptides were characterized by mass spectrometry.

### 2.2. Identification of the interactive surface of HR2 for binding with the HR1 core

The inhibitory potency of HR2 peptides against the six-helix bundle formation of FIV gp40 was examined by an ELISA (Table 1).<sup>12</sup> Two peptides **4a** and **5** exhibited higher inhibition compared with the parent peptide **3a** [ $IC_{50}$ (**3a**) = 708 nM;  $IC_{50}$ (**4a**) = 16.6 nM;  $IC_{50}$ (**5**) = 169 nM], whereas peptide **6** did not inhibit the interaction even at 10  $\mu$ M. HIV fusion inhibitors C34 **1** and SC35EK **2** showed no inhibition. These results indicate that the FIV HR2 sequence may interact with the HR1 coiled-coil via the residues positioned at *a/b/e* and/or *a/d/e*. On the other hand, FIV-mediated syncytium formation and FIV replication were blocked by treatment with peptides **3a** and **4a**, but not by peptides **5** and **6**.<sup>13</sup> Inhibition of the HR1–HR2 interaction by peptide **5** did not lead to anti-FIV activity suggesting that residues at *d* position are required for the interaction with HR1 of FIV gp40.

In order to rationalize the relationship between bioactivity and the conformations of the HR2 peptides, circular dichroism (CD) spectra were measured for peptides **3a**, **4a**, **5** and **6** in the absence or presence of the HR1 peptide. Negative ellipticities around 208 and 222 nm indicate the presence of a stable  $\alpha$ -helix structures for peptides **4a** and **5** in the absence of the HR1 peptide (Fig. 2a). In contrast, although the  $\alpha$ -helix inducible motifs were included, a random structure was observed for peptide **6**. The CD spectrum

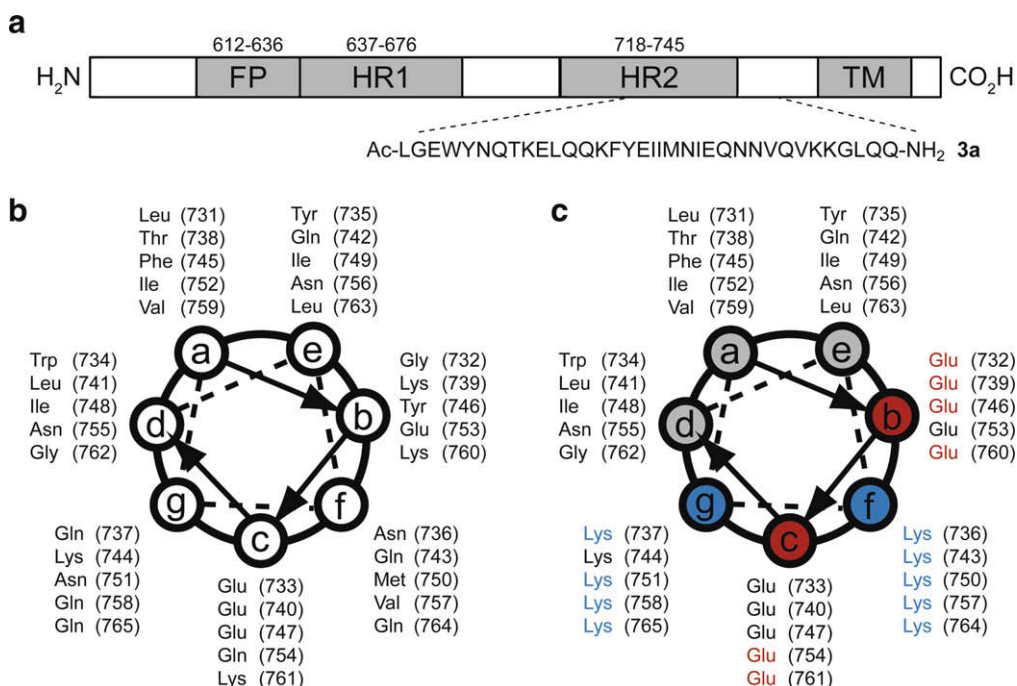


**Figure 1.** Design of FIV fusion inhibitors. (a) Schematic representation of FIV-1 gp40. The helical wheel representation of the HR2 peptide of FIV-1 gp40: (b) peptide **3a** and (c) peptide **4a**. FP: fusion peptide; HR1: heptad repeat-1; HR2: heptad repeat-2; TM: transmembrane domain.

**Table 1**  
Sequences and bioactivity of HR2-derived peptides of HIV-1 and FIV.

Peptide	Sequence	IC <sub>50</sub> (nM) <sup>a</sup>
<i>HIV-1</i>		
1 (C34)	WMEWDREINNYTSLIHLIEESQNQQEKNEQELL	>10,000
2 (SC35EK)	WEWDKKIEEYTKIEELIKKSEEQKKNEELKK	>10,000
<i>FIV</i>		
3a	LGEWYNQTKELQKQFYIEIMNIEQNNVQVKGLQQ	708
4a	LEEWYKKTTELQKKFEEIKKIEENNNKVEEGLKK	16.6
5	NEELGKKYEEETKKQEEFYKKIEIEKKNEEVKKLEELQKK	169
6	GEETLKKWEQTKKLEEFKKIEENIKKNEEQVKKGEEQLKK	>10,000

<sup>a</sup>IC<sub>50</sub> was determined as the concentration that blocked HR1–HR2 interaction by 50% in an ELISA.

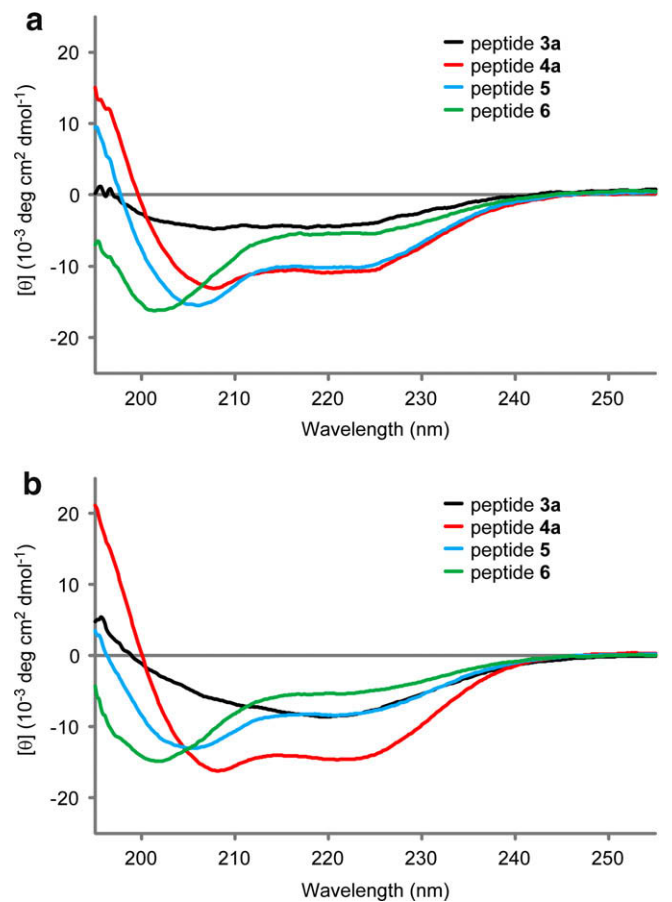


**Figure 2.** Circular dichroism spectra of HR2 peptides **3a**, **4a**, **5** and **6** in the presence (a) and absence (b) of the HR1 peptide.

of peptide **4a** in the presence of the HR1 peptide showed a slight enhancement of  $\alpha$ -helix conformation compared with the theoretical spectrum of the mixture without the interaction between HR1 and HR2 (Fig. 2b). This observation suggests that a stable six-helix bundle structure was formed between HR1 peptide and **4a**. The other HR1–HR2 mixtures did not indicate any enhancement in  $\alpha$ -helix content, which is correlated with the results obtained by a replication assay.<sup>13</sup> As such, it was demonstrated that residues at positions *a/d/e* of peptide **4a** provide the most appropriate interactive surface required for designing inhibitors against FIV infection (Fig. 1c).

**2.3. Structure–activity relationship for designing potent fusion inhibitors against multiple FIV strains**

The inhibitory potency of the anti-FIV HR2 peptides is affected by both the interactive surface and the stabilized  $\alpha$ -helix conformations supported by the arrangement of residues exposed to the aqueous solvent. Since the  $\alpha$ -helix content and stability of the peptide was enhanced by the X–EE–XX–KK motifs, the *a*, *d* and *e* positions could be further optimized for improving binding affinity. In addition, considering the clinical application against feline immunodeficiency, inhibitors that potently suppress broad range of FIV strains are favorable. Next, comparative inhibition of analogous peptides **3a–d** (native sequences) and **4a–d** (remodeled sequences) derived from several FIV strains was examined against potential formation of the six-helix bundles (Tables 2 and 3). Noticeably, peptide **3d** from the Shizuoka strain (clade D) contains ten different residues from **3a** (UK8) and **3c** (Sendai-1), and nine from **3b** (Petaluma). In contrast, there are only three differences in residue type observed among remodeled peptides **4a–d**, suggesting that the potential interactive residues are conserved among the four FIV strains.

ELISA with gp40 fragments derived from each strain was performed. Peptides **4a–d** with  $\alpha$ -helix inducible motifs exhibited higher potency of inhibition compared with the native sequences **3a–d**. FIV-mediated syncytium formation was also inhibited by peptides **3b** and **4b** (Fig. 3). Sendai-1-derived peptides **3c** and **4c** were less potent compared with the other peptides, suggesting that the N26S substitution on the interactive surface results in a decrease in the affinity towards the HR1 peptide. In contrast, the Shizuoka sequence provided the most potent peptides **3d** and **4d** against all strains. The potent bioactivity was attributed to a combination of Gly and Leu at the positions 29 and 33, respectively. Accordingly, the exposure of appropriate residues on the HR2 interactive surface such as the Shizuoka strain-derived peptide **4d** provide optimized inhibition against the formation of the six-helix bundle.

Comparative CD analysis demonstrated that the sequences of the HR1 peptide apparently influence the structures of the six-helix bundles (Fig. 4a). In contrast, peptides **4a–d** in the presence of an HR1 peptide derived from each strain exhibited similar six-helix bundle structures (Fig. 4b and Supplementary data).<sup>14</sup> These observations suggest that the binding affinity between the viral HR1 peptide and the inhibitory HR2 peptide would be determined primarily by the sequence of the viral HR1 peptide when the HR2 sequence was simplified by the incorporation of  $\alpha$ -helix inducible motifs.

**Table 2**  
Sequences of HR2-derived peptides of four FIV strains.

Peptide	Sequence <sup>a</sup>
<i>clade A</i>	
UK8	<b>3a</b> LGEWYNQTKELQKQFYIEIMNIEQNNVQVKGLQQ
	<b>4a</b> LEEWYKKTTELQKKFEEIKKIEENNNKVEEGLKK
Petaluma	<b>3b</b> LGEWYNQTKDLQKQFYIEIMDIEQNNVQKKGIQQ
	<b>4b</b> LEEWYKKTTELQKKFEEIKKIEENNNKVEEGLKK
Sendai-1	<b>3c</b> LGEWYNQTKGLQKQFYIEIMDIEQNSVQKKGIQQ
	<b>4c</b> LEEWYKKTTELQKKFEEIKKIEENNNKVEEGLKK
<i>clade D</i>	
Shizuoka	<b>3d</b> LRDWYNNQQLQKQFYIEIYDIEQNNVQKKGLQQ
	<b>4d</b> LEEWYKKTTELQKKFEEIKKIEENNNKVEEGLKK

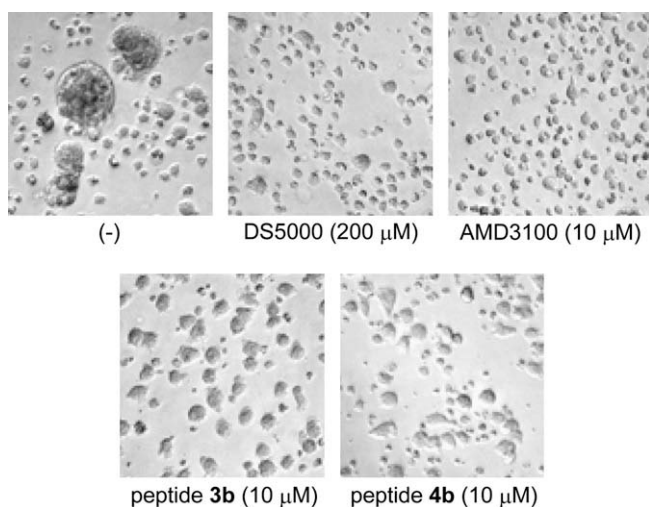
<sup>a</sup>The different residues in peptides **4b–d** from peptide **4a** are marked in green.

**Table 3**

Inhibitory activity of HR2-derived peptides against the HR1–HR2 interaction of four FIV strains

Peptide	IC <sub>50</sub> (nM, ELISA) <sup>a</sup>			
	UK8	Petaluma	Sendai-1	Shizuoka
<b>3a</b>	724	708	646	6310
<b>3b</b>	513	1260	183	6310
<b>3c</b>	>10,000	2400	437	>10,000
<b>3d</b>	182	195	37.2	2510
<b>4a</b>	5.39	16.6	22.6	115
<b>4b</b>	9.33	51.6	8.87	78.5
<b>4c</b>	443	200	42.4	203
<b>4d</b>	3.38	12.8	2.53	19.7

<sup>a</sup> IC<sub>50</sub> was determined as the concentration that blocked HR1–HR2 interaction by 50% in an ELISA.

**Figure 3.** Inhibition of FIV-mediated cell fusion by peptides **3b** and **4b**.

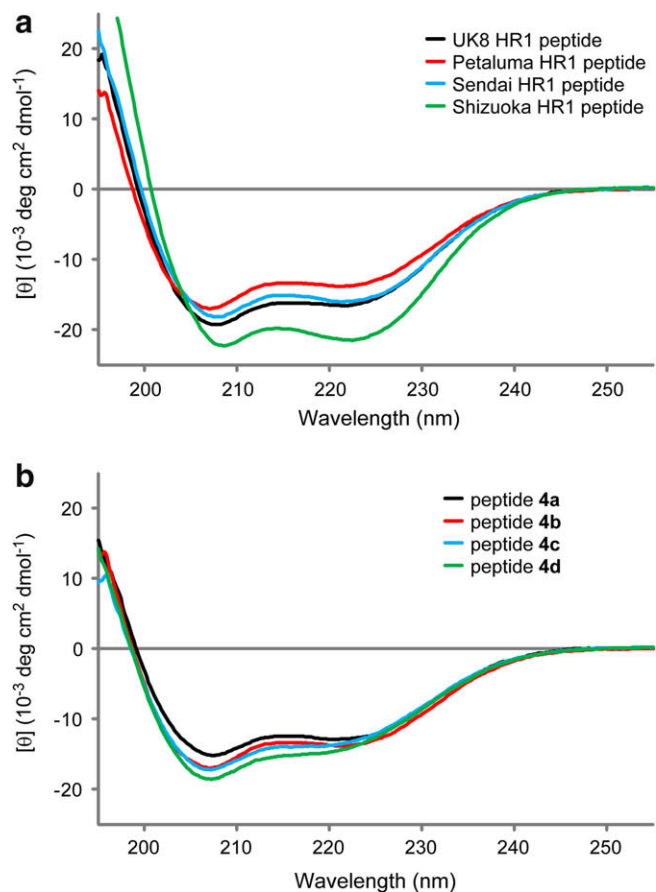
### 3. Conclusions

The current study investigated the use of an  $\alpha$ -helix inducible X–EE–XX–KK motif to stabilize the interaction between HR2 and the HR1 coiled-coil of the FIV gp40 protein. The most appropriate interactive surface on the HR2 peptide to provide potent inhibition appeared in the remodeled peptide **4a**, which was designed on the basis of the alignment with the HIV-1 gp41 HR2 sequence. Comparative analysis of HR2 peptides derived from several strains indicated that the most potent inhibition was provided by the interactive residues of the Shizuoka strain-derived peptide **4d**. As such, replacement of the solvent accessible residues with arranged Glu and Lys residues facilitated the optimization process of the interactive residues for high affinity binding on to the HR1 structure. Since class I virus fusion proteins share a high degree of structural homology and similar molecular mechanisms, the current approach may be useful in designing fusion inhibitors against other related viruses.

### 4. Experimental

#### 4.1. Peptide synthesis

Protected peptide-resins were manually constructed by Fmoc-based solid-phase peptide synthesis on NovaSyn® TGR resin (0.26 mmol/g, 385 mg, 0.1 mmol). *t*-Bu ester for Asp and Glu; 2,2,4,6,7-pentamethyldihydrobenzofuran-5-sulfonyl (Pbf) for Arg; *t*-Bu for Thr, Tyr and Ser; Boc for Lys; and Trt for Gln, Asn and His were employed for side-chain protection. Fmoc-amino acids were coupled using Fmoc-amino acid (0.5 mmol), *N,N'*-diisopro-

**Figure 4.** Circular dichroism spectra of (a) peptide **4a** in the presence of HR1 peptides (four strains) and (b) peptides **4a–d** in the presence of the HR1 peptide (Petaluma strain).

pylcarbodiimide (DIC, 0.077 mL, 0.5 mmol) and HOBt·H<sub>2</sub>O (77 mg) in DMF for 1.5 h. Fmoc deprotection was performed with 20% piperidine in DMF for 20 min. After N-terminal acetyl capping by treatment with Ac<sub>2</sub>O (0.050 mL)–pyridine (0.050 mL), the protected resin (200 mg) was treated with TFA/thioanisole/*m*-cresol/1,2-ethanedithiol/H<sub>2</sub>O (80:5:5:5:5, 2.5 mL) at room temperature for 2 h. After removal of the resin by filtration, the filtrate was poured into ice-cold dry Et<sub>2</sub>O. The resulting powder was collected by centrifugation and washed with ice-cold dry diethyl ether. Purification of the crude product by preparative HPLC on a Cosmosil 5C18-ARII preparative column (Nacalai Tesque, 20 × 250 mm) afforded the expected peptides. All peptides were characterized by an ESI-MS (Sciex APIIIIIE, Toronto, Canada) or MALDI-TOF-MS (AXIMA-CFR plus, Shimadzu, Kyoto, Japan), and the purity was calculated as >95% by HPLC on a Cosmosil 5C18-ARII analytical column (Nacalai Tesque, 4.6 × 250 mm) at 220 nm absorbance. The MS data are shown in [Supplementary data](#).

#### 4.2. FIV syncytial assay<sup>15</sup>

3201/FIV cells (2 × 10<sup>4</sup> cells/well) and MT-2 cells (1 × 10<sup>3</sup> cells/well) were seeded into 96-well plates with each peptide (10 μM). After 7 days, the cells were fixed with 1% formaldehyde and were examined using a BioZERO microscope (BZ-8000; Keyence, Osaka, Japan).

#### 4.3. ELISA-based competition assay

Recombinant purified MBP-HR1 dissolved in 50 mM sodium carbonate buffer (pH 8.5) was coated on a 96-well ELISA plate

(Costar, Cambridge, MA) by incubation at 4 °C for 12 h. After washing three times with PBS containing 0.25% Tween 20 (T-PBS), the plate was blocked using bovine serum albumin (BSA) at a concentration of 1 mg/mL in T-PBS at 4 °C for 2.5 h, and then washed again as described above. The MBP-HR1 was allowed to bind biotinylated HR2 peptide (peptide **3**, 120 nM) by incubation at 37 °C for 1.5 h in the presence or absence of various concentrations of the test peptides. After washing, binding of biotin-HR2 peptide was detected using streptavidin alkaline phosphatase (CALBIO-CHEM) using a 1:5000 dilution at 4 °C for 1 h. Subsequently, this reaction was washed as before, prior to the addition of the phosphatase substrate 5-bromo-4-chloro-3-indolyl phosphate (BCIP) (BluePhos Microwell Phosphatase Substrate; KPL, Gaithersburg, MD). After incubating at room temperature for 25 min, the absorbance at 595 nm was measured using a plate reader (Model 3550, Bio-Rad).

#### 4.4. Measurement of CD spectra

The HR2 peptide was dissolved in PBS (pH 7.4) at a concentration of 10  $\mu$ M. The mixture of the selected HR1 and HR2 peptides was incubated at 37 °C for 30 min prior to the CD measurement (the final concentration of both HR1 and HR2 peptides was 10  $\mu$ M in PBS, pH 7.4). The wavelength-dependent molar ellipticity  $[\theta]$  was monitored at 25 °C as the average of eight scans, and the thermal stability of the HR1 and HR2 mixture was estimated by monitoring the change in the CD signal at 222 nm in a spectropolarimeter (Model J-710; Jasco, Tokyo, Japan). The midpoint of the thermal unfolding transition of each complex was defined as the melting temperature ( $T_m$ ).

#### Acknowledgments

This work was supported by the Science and Technology Incubation Program in Advanced Regions from the Japan Science and Technology Agency, Grants-in-Aid for Scientific Research from the Ministry of Education, Culture, Sports, Science, and Technology of Japan, and Health and Labour Sciences Research Grants (Research on HIV/AIDS). H.N. is grateful for the JSPS Research Fellowships for Young Scientists.

#### Supplementary data

Supplementary data associated with this article can be found, in the online version, at [doi:10.1016/j.bmc.2009.06.001](https://doi.org/10.1016/j.bmc.2009.06.001).

#### References and notes

- Dunham, S. P.; Graham, E. *Vet. Clin. Small Anim. Pract.* **2008**, *38*, 879.
- Fletcher, N. F.; Brayden, D. J.; Brankin, B.; Callanan, J. J. *Vet. Immunol. Immunopathol.* **2008**, *123*, 134.
- (a) Wyatt, R.; Sodroski, J. *Science* **1998**, *280*, 1884; (b) Garg, H.; Fuller, F. J.; Tompkins, W. A. *Virology* **2004**, *321*, 274; (c) Elder, J. H.; Sundstrom, M.; De Rozieres, S.; De Parseval, A.; Grant, C. K.; Lin, Y. C. *Vet. Immunol. Immunopathol.* **2008**, *123*, 3.
- (a) Shimojima, M.; Miyazawa, T.; Ikeda, Y.; McMonagle, E. L.; Haining, H.; Akashi, H.; Takeuchi, Y.; Hosie, M. J.; Willett, B. J. *Science* **2004**, *303*, 1192; (b) De Parseval, A.; Chatterji, U.; Sun, P.; Elder, J. H. *Proc. Natl. Acad. Sci. U.S.A.* **2004**, *101*, 13044.
- (a) Willett, B. J.; Hosie, M. J.; Neil, J. C.; Turner, J. D.; Hoxie, J. A. *Nature* **1997**, *385*, 587; (b) Richardson, J.; Pancino, G.; Merat, R.; Leste-Lasserre, T.; Moraillon, A.; Schneider-Mergener, J.; Alizon, M.; Sonigo, P.; Heveker, N. J. *Virology* **1999**, *73*, 3661.
- (a) Egberink, H. F.; De Clercq, E.; Van Vliet, A. L.; Balzarini, J.; Bridger, G. J.; Henson, G.; Horzinek, M. C.; Schols, D. J. *Virology* **1999**, *73*, 6346; (b) Mizukoshi, F.; Baba, K.; Goto-Koshino, Y.; Setoguchi-Mukai, A.; Fujino, Y.; Ohno, K.; Tamamura, H.; Oishi, S.; Fujii, N.; Tsujimoto, H. J. *Vet. Med. Sci.* **2009**, *71*, 121.
- Kiellian, M.; Rey, F. A. *Nat. Rev. Microbiol.* **2006**, *4*, 67.
- Matthews, T.; Salgo, M.; Greenberg, M.; Chung, J.; DeMasi, R.; Bolognesi, D. *Nat. Rev. Drug Discovery* **2004**, *3*, 215.
- (a) Lombardi, S.; Massi, C.; Indino, E.; La Rosa, C.; Mazzetti, P.; Falcone, M. L.; Rovero, P.; Fissi, A.; Pieroni, O.; Bandecchi, P.; Esposito, F.; Tozzini, F.; Bendinelli, M.; Garzelli, C. *Virology* **1996**, *220*, 274; (b) Medinas, R. J.; Lambert, D. M.; Tompkins, W. A. *J. Virol.* **2002**, *76*, 9079; (c) D'Ursi, A. M.; Gianecchini, S.; Di Fenza, A.; Esposito, C.; Armenante, M. R.; Carotenuto, A.; Bendinelli, M.; Rovero, P. *J. Med. Chem.* **2003**, *46*, 1807; (d) Gianecchini, S.; Di Fenza, A.; D'Ursi, A. M.; Matteucci, D.; Rovero, P.; Bendinelli, M. *J. Virol.* **2003**, *77*, 3724; (e) Gianecchini, S.; Alcaro, M. C.; Isola, P.; Sichi, O.; Pistello, M.; Papini, A. M.; Rovero, P.; Bendinelli, M. *Antiviral Ther.* **2005**, *10*, 671; (f) D'Ursi, A. M.; Gianecchini, S.; Esposito, C.; Alcaro, M. C.; Sichi, O.; Armenante, M. R.; Carotenuto, A.; Papini, A. M.; Bendinelli, M.; Rovero, P. *ChemBiochem.* **2006**, *7*, 774.
- (a) Otake, A.; Nakamura, M.; Nameki, D.; Kodama, E.; Uchiyama, S.; Nakamura, S.; Nakano, H.; Tamamura, H.; Kobayashi, Y.; Matsuoka, M.; Fujii, N. *Angew. Chem., Int. Ed.* **2002**, *41*, 2937; (b) Oishi, S.; Ito, S.; Nishikawa, H.; Watanabe, K.; Tanaka, M.; Ohno, H.; Izumi, K.; Sakagami, Y.; Kodama, E.; Matsuoka, M.; Fujii, N. *J. Med. Chem.* **2008**, *51*, 388; (c) Nishikawa, H.; Oishi, S.; Fujita, M.; Watanabe, K.; Tokiwa, R.; Ohno, H.; Kodama, E.; Izumi, K.; Kajiwar, K.; Naitoh, T.; Matsuoka, M.; Otake, A.; Fujii, N. *Bioorg. Med. Chem.* **2008**, *16*, 9184; (d) Nishikawa, H.; Nakamura, S.; Kodama, E.; Ito, S.; Kajiwar, K.; Izumi, K.; Sakagami, Y.; Oishi, S.; Ohkubo, T.; Kobayashi, Y.; Otake, A.; Fujii, N.; Matsuoka, M. *Int. J. Biochem. Cell Biol.* **2009**, *891*; (e) Naitoh, T.; Izumi, K.; Kodama, E.; Sakagami, Y.; Kajiwar, K.; Nishikawa, H.; Watanabe, K.; Sarafianos, S. G.; Oishi, S.; Fujii, N.; Matsuoka, M. *Antimicrob. Agent Chemother.* **2009**, *53*, 1013.
- Singh, M.; Berger, B.; Kim, P. S. *J. Mol. Biol.* **1999**, *290*, 1031.
- Nishikawa, H.; Kodama, E.; Sakakibara, A.; Fukudome, A.; Izumi, K.; Oishi, S.; Fujii, N.; Matsuoka, M. *Antiviral Res.* **2008**, *80*, 71.
- Mizukoshi, F.; Baba, K.; Goto, Y.; Setoguchi, A.; Fujino, Y.; Ohno, K.; Oishi, S.; Kodera, Y.; Fujii, N.; Tsujimoto, H. *Vet. Microbiol.* **2009**, *136*, 155.
- The similar thermal stabilities of the potential six-helix bundle structures were also observed. For example, the melting temperatures ( $T_m$ ) of peptides **4c** and **4d** in the presence of UK8 strain-derived HR1 peptide were 57.1 °C and 54.7 °C, respectively. Unfortunately, we were not able to get clearer physicochemical proofs of the lower bioactivity of the Sendai strain-derived peptide **4c**.
- Tanabe-Tochikura, A.; Tochikura, T. S.; Blakeslee, J. R., Jr.; Olsen, R. G.; Mathes, L. E. *Antiviral. Res.* **1992**, *19*, 161.